PASJ: Publ. Astron. Soc. Japan **46**, L167–L171 (1994)

An ASCA Observation of the Seyfert 2 Galaxy Markarian 3

Kazushi IWASAWA,[1] Tahir YAQOOB,[2*] Hisamitsu AWAKI,[3] and Yasushi OGASAKA[4]

[1] *Department of Astrophysics, Nagoya University, Chikusa-ku, Nagoya 464-01*
[2] *NASA/Goddard Space Flight Center, Greenbelt, MD20771, USA*
[3] *Department of Physics, Kyoto University, Sakyo-ku, Kyoto 606-01*
[4] *The Institute of Space and Astronautical Science, Yoshinodai, Sagamihara, Kanagawa 229*

(Received 1993 December 13; accepted 1994 August 9)

Abstract

We report preliminary results of an ASCA observation of the Seyfert 2 galaxy Mkn 3. Comparison with previous Ginga and BBXRT observations shows that the observed hard X-ray luminosity above 4 keV decreased by a factor of ~ 3 (intrinsic luminosity by almost a factor of 6) in a period of ~ 3.6 yr. On the other hand, the soft luminosity has not varied significantly in ~ 13 yr, lending support to the extended nature of the soft emission, perhaps dominated by scattering of the nuclear X-rays. ASCA resolves the Fe K line emission into at least two components for the first time. The dominant component at 6.4 keV has an equivalent width of ~ 860 eV and FWHM $\sim 10^4$ km s^{-1}, while the second component has an equivalent width of ~ 190 eV and appears to be narrower than the first. The total intensity of the Fe K emission decreased by factor of over 3 in response to the decrease in the continuum level, implying that a substantial part of the dominant Fe K emission must originate in a region smaller than that responsible for the soft emission. The variability provides direct evidence that the hard X-ray continuum and Fe K line in this Seyfert 2 are being observed *directly* through the nuclear obscuring material, not in scattered light.

Key words: Galaxies: active — Galaxies: individual (Mkn 3) — Galaxies: nuclei — X-rays: galaxies

1. Introduction

Studies of the X-ray spectra of Seyfert 2 galaxies in the hard X-ray band with Ginga (> 2 keV) generally show power-law spectra similar to Seyfert 1 galaxies (e.g., Awaki et al. 1991). Often there is an Fe K line at ~ 6.4 keV imprinted on the continuum and a heavy low-energy cut-off due to obscuration. These characteristics have been taken as support for the so-called "unification scheme" whereby Seyfert 2 nuclei are simply Seyfert 1 nuclei seen in scattered light, the direct emission being blocked by an obscuring torus which also hides the Broad Line Region (BLR). Soft X-ray observations (e.g., with ROSAT, see Mulchaey et al. 1993; Turner et al. 1993), which show the absorbed spectra to rise again below ~ 1 keV or so, lend further support to this idea since this emission is interpreted as originating in the scattering zone—a key component of the unified model (e.g., see Krolik, Kallman 1987). Unlike Seyfert 1 nuclei, little is known about the short or long term X-ray variability of Seyfert 2 nuclei. The X-ray emission is weak compared to Seyfert 1 types so requires high sensitivity to study short term variability Seyfert 2 nuclei have simply not been observed often enough to monitor longer term variability. Detection of significant variability would indeed strengthen the view that Seyfert 2 nuclei really are not different to Seyfert 1 nuclei.

Mkn 3 ($z = 0.0137$) is one of the prototype Seyfert 2 galaxies with polarized broad emission lines (Miller, Goodrich 1990). An observation with Ginga (Awaki et al. 1990, 1991) revealed a powerful hard X-ray source ($L_{2-10\mathrm{keV}} = 4 \times 10^{43}$ erg s^{-1} corrected for absorption; $H_0 = 50$ km s^{-1} Mpc^{-1} and $q_0 = 0$ is assumed throughout this paper) with a significant column density of $N_{\mathrm{H}} \simeq 7 \times 10^{23}$ cm^{-2} obscuring an underlying power-law continuum with a photon index, Γ, of 1.5. In the soft X-ray band the Einstein IPC (Kruper et al. 1990) and ROSAT PSPC (Turner et al. 1993) spectra lie well above the extrapolation of the obscured hard continuum. A strong Fe K line at 6.4 keV with an equivalent width of ~ 550 eV was found by Ginga and also by BBXRT (Marshall et al. 1992) with similar energy and equivalent width. The shape of the continuum across the transition of the hard to soft emission components, the structure and origin of the Fe K line and the possible existence of other, previously unresolved line-emission components have remained outstanding issues which can now be addressed with ASCA.

* With the Universities Space Research Association.

2. Observation and Data Reduction

A summary of the ASCA mission and focal-plane detectors can be found in Tanaka et al. (1994). Mkn 3 was observed by ASCA on 1993 April 21 with the SIS operating in 4-CCD mode. Events were extracted from circular regions of radius $\sim 2'$–$3'$ for the SIS and $\sim 3'$–$4'$ for the GIS. In this analysis we use SIS data from only one chip in each sensor which contains by far the majority of source counts. For the SIS, background events were extracted from parts of the chip sufficiently offset from the source whilst for the GIS annular rings centered on the source were used. The total extracted count rates are $\sim$ 0.05–0.08 ct s^{-1} in the four instruments. The background in each source region constitutes $\sim$ 8% of the total count rate in the SIS and $\sim$ 15% in the GIS. No significant variability of the source count rates within the observation could be detected though the statistics are too poor to rule out short-term variability. Events in SIS FAINT and BRIGHT mode were combined. Spectra from the cleaned source and background events resulted in exposure times ranging from ~ 3.2–3.3×10^4 s for S0 and S1 respectively and $\sim 3.8 \times 10^4$ s for S2 and S3. Since current uncertainties in exposure corrections make it difficult to obtain absolute SIS fluxes, we use mean normalizations from S2 and S3 to estimate fluxes, using flux ratios in S0 and S1 where necessary.

In both GIS and SIS images, a weak source, 2E 0607+7108 (BL Lac object MS 0607.9+7108 at $z = 0.267$) was detected at 10.′6 NW of Mkn 3 with a count rate of $\sim$ 0.007 ct s^{-1}. The spectrum can be described by an unabsorbed power law with $\Gamma = 2.4$ (90%, 1 parameter confidence range of 1.9–3.0). In a ROSAT PSPC image, Turner et al. (1993) discovered a weak companion source located at 1.′8 W of Mkn 3. In the ASCA S0 image, a possible source is found at the ROSAT position. In S1 the source falls in an inter-chip gap. We estimate that the X-ray flux of this companion source constitutes only $\sim$ 4% of the total flux (including Mkn 3) in the 0.1–2.0 keV band (Turner et al. 1993). Including it in the analysis will not affect the conclusions of this paper.

3. Spectral Fitting Results

3.1. Broadband Fits

In this initial part of the analysis, designed to give an overall view of the X-ray emission, we bin the spectra to have greater than 20 count per bin and subtract the background directly, allowing use of χ^2 for parameter minimization. A simple absorbed power-law model is inadequate to describe the broadband SIS data because of the 'excess' soft flux. The data from all four instruments were fitted simultaneously with the simplest extension of the above model in which a fraction of the same power-law continuum is allowed to escape only to be absorbed by the Galactic column of 8.7×10^{20} cm^{-2} (Stark et al. 1992). The unabsorbed component can be interpreted as that part of the direct continuum which is scattered into our line-of-sight in the same extended electron-scattering zone which is thought to scatter lines from the hidden BLR into our line-of-sight. The data, best-fitting model ($\Gamma \sim 2.2$) and ratios of data to model are shown in figure 1a (SIS) and 1b (GIS). Although the fit is simultaneous, the SIS and GIS data are separated for clarity. Immediately apparent from figure 1 is that the fit is very poor but quite remarkable, with a rich variety of line-like features present across the entire spectrum. The line features are much clearer in the SIS due to the smearing which results from a poorer energy resolution of the GIS. However a very prominent Fe feature between 6–7 keV is clear in both SIS and GIS. In the SIS, the bump below 1.5 keV peaked at 0.9 keV can be interpreted as an emission-line blend of various L-shell transitions of Fe XVII–Fe XXIV, Ne IX–Ne X Kα, and Mg XI Kα from thermal or photoionized plasma. The inclusion of a cosmic abundance Raymond-Smith model to the S0+S1 data results in $kT = 0.80^{+0.07}_{-0.10}$ keV and improves the fit by $\Delta\chi^2 = 20$. A flatter power-law continuum is obtained with $\Gamma = 1.77^{+0.32}_{-0.14}$ and the absorbing column becomes $N_{\rm H} = 4.9^{+1.7}_{-1.2} \times 10^{23}$ cm^{-2}. However, those significant line-like residuals at 0.75 keV, 1.3 keV, 1.85 keV, 2.3 keV, 3.0 keV, and 3.9 keV still remain which we can identify with a blend of O VIII and Fe XVII, highly ionized Mg, Si, S, Ar, and Ca Kα. This indicates that the emission lines might arise in photoionized gas rather than collisionally ionized plasma. Typical equivalent widths of these lines lie in the range $\sim 50 - 120$ eV (obtained from fitting with Guassians in addition to the power-law plus scattering model). We note that caution must be excercised in interpreting features around 2 keV since there are known artifacts in the instrumental responses around this energy.

Detailed modelling of the continuum and emission-line spectrum of Mkn 3 will be presented in future work. In particular, we note that our representation of the scattered continuum, with the same photon index as the direct continuum, is surely too simple. Self-consistent photoionization models which include scattering are required here. As for the direct continuum, an inherent limitation of the ASCA data is that the complexity of the spectrum means we cannot get a good handle on Γ, which not only depends on the model, but the energy range used for spectral fitting. Further complication could result if there is a reflection component present as is found in a number of Seyfert 1 galaxies which could account for the rather flat power-law index of 1.5 measured by Ginga, compared with that for typical Seyfert 1's (e.g., Nandra, Pounds 1994). However, ASCA is not so sensitive to the reflection component unless it dominates the spectrum.

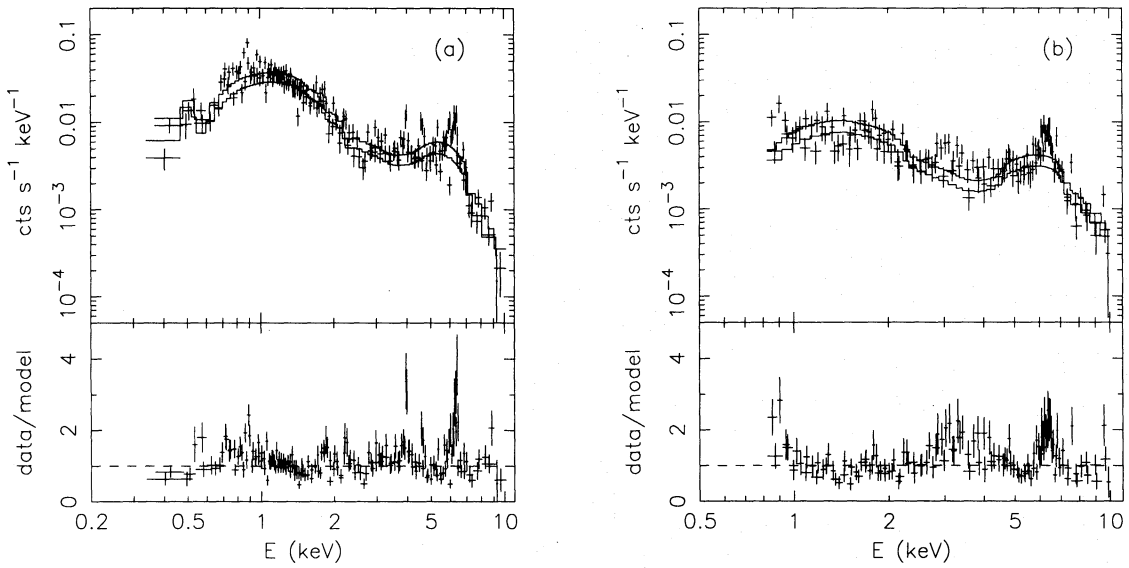

Fig. 1. The data, best-fitting simple scattering plus absorption model and the ratios of data to model for the four instrument, simultaneous fitting. The SIS data (a) are shown separated from the GIS data (b) for clarity.

In summary, however we model the soft X-ray continuum, the ASCA data are consistent with a direct power-law index in the range $\Gamma \sim 1.5-2.0$ with a corresponding absorbing column in the range ~ 3–7×10^{23} cm^{-2}.

From the model-fitting described above we estimate the observed 0.5–4 keV flux to be 8.2×10^{-13} erg cm^{-2} s^{-1}. This is comparable to previous measurements with the Einstein IPC (Kruper et al. 1989), BBXRT (Marshall et al. 1992), and the ROSAT PSPC (Turner et al. 1993). In the remainder of the paper we will concentrate on the Fe K emission so we restrict the analysis to the data above 1 keV in order to avoid a possible 'ultra-soft' component.

3.2. The Hard X-Rays and Fe K Emission

Figure 2 shows the data from the four instruments at a finer resolution, in the 4.5–8 keV band, in order to show the structure in the Fe K feature (without background subtraction). Note that the S0 and S1 data appear to be qualitatively different. We have checked that this is not due to gain-shift problems by fitting the SIS background spectra from offset parts of the chip and confirming that the prominent fluorescence lines in the background are at the expected energies (see Gendreau et al. 1994). The differences must be statistical. Preliminary spectral fitting to data from individual instruments with the scattering model described above plus Gaussian line-components using the maximum likelihood statistic, the unbinned data in the 1–10 keV band, and models of the local background confirmed what is evident by eye from figure 2. Namely, there is a dominant emission component centered at $\sim$ 6.4 keV in the source frame and another, marginally significant component, at $\sim$ 7 keV (source frame). The energy of the latter appears to be lower in S1 and S3 than in S0 and S2. In S0 there appears to be a third component at 6.15 keV (source frame) which is significant at greater than 90% confidence. However, the feature is not significant in any of the other instruments. Note that the peak at $\sim$ 5.7 keV in S1 is *not* the same feature but is likely to be a statistical artifact. Unfortunately the statistics of the data are so poor that none of the line parameters, including equivalent widths, can be well constrained from the individual fits. As a step towards maximizing the statistics by simultaneously fitting four instruments, we repeated the individual fits using data binned with a minimum of 20 count per bin and the χ^2 statistics with background subtraction. We obtained completely consistent results since, between $\sim$ 6–7 keV, typically only 3 bins at a time are combined together. No having to model the background overcomes considerable technical difficulties in multi-instrument fitting. Thus we perform a four-instrument fit with the scattering model, first including only one Gaussian to model the dominant Fe K emission. The center energy (E_1), intrinsic width (σ_1), and equivalent width (EW_1) are allowed to float. The addition of another Gaussian component to model the feature at $\sim$ 7 keV, with intrinsic width initially fixed at 0.01 keV, reduces χ^2 by only 8.1 (significance $> 90\%$ for 2 parameters). Next the intrinsic width of this component is allowed to float also but turns out to be less than 0.01 keV. The results are shown in full in table 1. Note that the addition of a third Gaussian component to

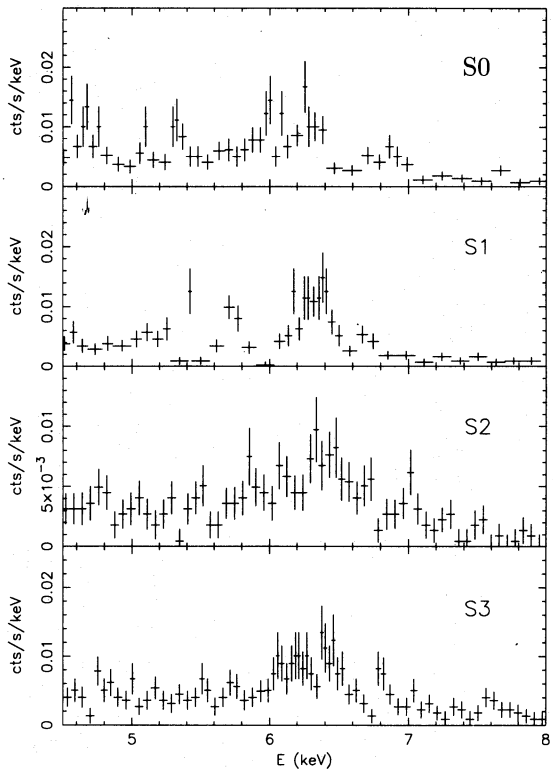

Fig. 2. The data from the four instruments in the 4.5–8 keV band showing the Fe K features in detail. No background has been subtracted.

Table 1. Four-instrument spectral fit in the 1–10 keV band with the scattering model including two Fe K line components.*

Γ	1.78 (1.63–1.95)
$N_{\rm H}$ (10^{23} cm^{-2})	4.42 (3.32–5.77)
$f_{\rm scat}$	0.106 (0.078 – 0.145)
Fe K $E_1^{\S}$ (keV)	6.43 (6.40–6.46)
Fe K σ_1 (keV)	0.094 (0.053–0.137)
Fe K $EW_1^{\dagger}$ (eV)	862 (556–1334)
Fe K $E_2^{\S}$ (keV)	7.05 (6.91–7.14)
Fe K σ_2 (keV)	0.002 (0.0–0.65)
Fe K $EW_2^{\dagger}$ (eV)	190 (43–392)

* Parentheses in values indicate 90% confidence intervals for two interesting parameters (see Lampton et al. 1976).
† *Observed* equivalent width.
§ Line energies are in the source frame.

account for the feature at ~ 6.15 keV in S0 surprisingly results in *no* decrease in χ^2 so the existence of this feature remains a mystery. Note that despite a good fit of the two Gaussian components to the Fe K feature, the overall fit still gives a poor χ^2 (401.5 for 255 d.o.f.). This is due mainly to several line-like features across the spectrum, but it does not alter the derived parameters on the Fe K line.

We estimate the observed 4–10 keV flux to be $\sim 2.7 \times 10^{-12}$ erg cm^{-2} s^{-1} which is a factor of ~ 3 lower than the Ginga value (8.8×10^{-12} erg cm^{-2} s^{-1}; Awaki et al. 1991). We can also compare the 2–10 keV absorption-corrected luminosity estimated from the ASCA data at 7.2×10^{42} erg s^{-1}, almost a factor of 6 lower than the Ginga value. The BBXRT observation made between the times of the Ginga and ASCA observations, measured an intermediate observed hard flux, a factor of 2 down on the Ginga value. The total equivalent width of the two Fe K emission components (~ 1.05 keV) is twice the total equivalent width of the unresolved emission measured by Ginga. We estimate the total observed *intensity* of the two Fe K components to be $\sim 4.5 \times 10^{-5}$ photon cm^{-2} s^{-1} ($\sim 9.1 \times 10^{-5}$ photon cm^{-2} s^{-1} corrected for absorption). Both the observed and intrinsic intensities are down by over a factor of 3 times compared to the respective Ginga values. The larger equivalent width in the ASCA observation compared to Ginga is easily understood in terms of the continuum level at 6.4 keV decreasing more than the line intensity. Also, table 1 shows that the fraction of the total flux scattered into our line-of-sight ($f_{\rm scat}$) is $\sim 11\%$, understandably higher than the $\sim 3\%$ estimated from BBXRT, given the non-variability of the soft flux.

4. Discussion

We have shown that the observed hard X-ray continuum in Mkn 3 above 4 keV decreased by almost a factor of ~ 3 (factor of ~ 6 for the intrinsic luminosity) in a ~ 3.6 yr interval, and this was not accompanied by changes in the softer flux. The large amplitude hard X-ray variability is typical of Seyfert 1 nuclei and provides direct evidence that the hard X-rays in this Seyfert 2 are observed directly through the putative obscuring torus, as suggested by Mulchaey et al. (1993) for other Seyfert 2's. The non-variability of the soft flux supports the idea that the soft emission originates in an extended region, perhaps dominates by scattering of the intrinsic continuum. The scattering medium is likely to be optically thin since there is little evidence of excess absorption in the soft X-ray spectrum. ASCA resolves the Fe K line into at least two components for the first time, the dominant one (identified with Fe K$_\alpha$) at ~ 6.4 keV (equivalent width ~ 860 eV) and the smaller one at ~ 7 keV (equivalent width ~ 190 eV). The fact that the intensity of the Fe K emission components decreased by over a factor of 3 when the continuum decreased means that a substantial part of the Fe K emission must originate in a region *smaller* than that responsible for the non-variable soft emission. The accompanying increase

in equivalent width may either be due to time lags or a non-varying component of the Kα line. The energy of the dominant emission component implies that it must originate in cool gas, much of which must be closer to the nucleus than the scattering region. Perhaps this component originates in the obscuring material itself (e.g., see Krolik et al. 1994). The FWHM of the '6.4 keV' line of $10.3^{+4.7}_{-4.5} \times 10^3$ km s^{-1} is actually typical of velocities in the BLR. However, narrow Fe K lines can also be produced by X-ray illuminated disks (as postulated for the origin of the Fe K line in Seyfert 1 galaxies), observed at small inclination angles. The large equivalent width would then have to be produced by the combined effects of absorption, scattering, and geometry. The second Fe K component at ~ 7 keV, also narrow, could be identified with Fe Kβ emission or Kα from Hydrogen-like iron. In the former case, the line ratio to the 6.4 keV line is about twice that expected from the simplest assumptions. The origin of this line will be investigated in future work. Intensive monitoring of this source is required to quantify variability timescales of the continuum and lines and relative lags in order to place tight constraints on the geometry and structure of the nucleus.

The authors thank all members of the ASCA team and the operations staff at ISAS. KI thanks JSPS for support of Young Scientists in the form of fellowships.

References

Awaki H., Koyama K., Kunieda H., Tawara Y. 1990, Nature 346, 544
Awaki H., Koyama K., Inoue H., Halpern J.P. 1991 PASJ 43, 195
Gendreau K. et al. 1994, PASJ submitted
Krolik J.H., Kallman T. 1987, ApJL 320, L25
Krolik J.H., Madau P., Zycki P.T. 1994, ApJL 420, L57
Kruper J.S., Urry C.M., Canizares C.R. 1990, ApJS 74, 347
Lampton M., Margon B., Bowyer S. 1976, ApJ 208, 177
Marshall F.E. et al. 1992, in Proc of Frontiers of X-ray Astronomy, ed Y. Tanaka, K. Koyama (UAP, Tokyo) p129
Miller J.S., Goodrich R.W. 1990, ApJ 355, 456
Mulchaey J.S., Colbert E., Wilson A.S., Mushotzky R.F., Weaver K.A. 1993, ApJ 414, 144
Nandra K., Pounds K.A. 1994, MNRAS 268, 405
Stark A.A., Gammie C.F., Wilson R.W., Bally J., Linke R. Heiles C., Hurwitz M. 1992, ApJS 79, 77
Tanaka Y., Inoue H., Holt S.S. 1994, PASJ 46, L37
Turner T.J., Urry C.M., Mushotzky R.F. 1993, ApJ 418, 653